

**OAK RIDGE
NATIONAL
LABORATORY**



**Verification Calculation Results to
Validate the Procedures and Codes for
Pin-by-Pin Power Computation
In VVER Type Reactors with
MOX Fuel Loading**

Authors

**Z. N. Chizhikova
A. G. Kalashnikov
E. N. Kapranova
V. E. Korobitsyn
G. N. Manturov
A. A. Tsiboulia**

This report has been reproduced from the best available copy.

Reports are available to the public from the following source.

National Technical Information Service
5285 Port Royal Road
Springfield, VA 22161
Telephone 703-605-6000 (1-800-553-6847)
TDD 703-487-4639
Fax 703-605-6900
E-mail orders@ntis.fedworld.gov
Web site <http://www.ntis.gov/ordering.htm>

Reports are available to U.S. Department of Energy (DOE) employees, DOE contractors, Energy Technology Data Exchange (ETDE) representatives, and International Nuclear Information System (INIS) representatives from the following source.

Office of Scientific and Technical Information
P.O. Box 62
Oak Ridge, TN 37831
Telephone 423-576-8401
Fax 423-576-5728
E-mail reports@adonis.osti.gov
Web site <http://www.osti.gov/products/sources.html>

Reports produced after January 1, 1996, are generally available via the DOE Information Bridge.

Web site <http://www.doe.gov/bridge>

This report was prepared as an account of work sponsored by an agency of the United States Government. Neither the United States Government nor any agency thereof, nor any of their employees, makes any warranty, express or implied, or assumes any legal liability or responsibility for the accuracy, completeness, or usefulness of any information, apparatus, product, or process disclosed, or represents that its use would not infringe privately owned rights. Reference herein to any specific commercial product, process, or service by trade name, trademark, manufacturer, or otherwise, does not necessarily constitute or imply its endorsement, recommendation, or favoring by the United States Government or any agency thereof. The views and opinions of authors expressed herein do not necessarily state or reflect those of the United States Government or any agency thereof.

**VERIFICATION CALCULATION RESULTS TO VALIDATE THE
PROCEDURES AND CODES FOR PIN-BY-PIN POWER COMPUTATION
IN VVER TYPE REACTORS WITH MOX FUEL LOADING
(American-Russian Benchmark, Variants 13, 14)**

Authors

Z. N. Chizhikova
A. G. Kalashnikov
E. N. Kapranova
V. E. Korobitsyn
G. N. Manturov
A. A. Tsiboulia

Date Published: December 1998

Report Prepared by
LOCKHEED MARTIN ENERGY RESEARCH CORP.
P.O. Box 2008
Oak Ridge, Tennessee 37831-6363
under
Subcontract Number 85B99398V

Funded by
Office of Fissile Materials Disposition
United States Department of Energy

Prepared for

Computational Physics and Engineering Division
Oak Ridge National Laboratory
Oak Ridge, Tennessee 37831
managed by
LOCKHEED MARTIN ENERGY RESEARCH CORP.
for the
U.S. DEPARTMENT OF ENERGY
under contract DE-96OR22464

**STATE SCIENTIFIC CENTRE OF RUSSIAN FEDERATION -
Leipunsky INSTITUTE OF PHYSICS AND POWER ENGINEERING**

**VERIFICATION CALCULATION RESULTS
TO VALIDATE THE PROCEDURES AND CODES
FOR PIN-BY-PIN POWER COMPUTATION
IN VVER TYPE REACTORS WITH MOX FUEL LOADING
(American-Russian benchmark, Variants 13, 14)**

SCIENTIFIC REPORT

Authors:

**Chizhikova Z.N.
Kalashnikov A.G.
Kapranova E.N.
Korobitsyn V.E.
Manturov G.N.
Tsiboulia A.A.**

Obninsk - 1998

ABSTRACT

INTRODUCTION	3
1. SPECIFICATION OF CALCULATIONAL BENCHMARKS	5
1.1. Material Specification	5
1.2. Geometry Description	5
1.3. A Set of States to Be Calculated	7
1.4. Parameters to Be Calculated	8
1.5. Description of Calculational Variants	8
2. BRIEF DESCRIPTION OF CALCULATIONAL CODES	9
2.1. MCU-B Code	9
2.2. Program-Constant Complex CONSIST-KENO-MAYAK-ORIGEN	11
2.3. Description of Methodical Basis of the TVS-M Code	14
2.4. HELIOS Code	16
2.5. Program Complex TRIANG-PWR	17
2.6. WIMS-ABBN	18
3. CALCULATION RESULTS	21
3.1. Comparison of the Calculation Results Obtained by the CONKEMO Code with Different Time Steps	22
3.2. Comparison of the K_{eff} Value Calculation Results	27
3.3. The Results of Power Distribution Calculations Using Benchmark Codes at the Beginning of Burnup	29
3.4. Comparison of the Calculations of Power Distributions on Burning Obtained by the TVS-M, HELIOS and CONKEMO Codes	34
3.5. The Statistical Error Estimate on Power Distribution Calculation by CONKEMO Code	63
3.6. Calculation Results Obtained by the TRIANG-PWR Code	66
CONCLUSION	76
REFERENCES	77

INTRODUCTION

One of the important problems for ensuring the VVER type reactor safety when the reactor is partially loaded with MOX fuel is the choice of appropriate physical zoning to achieve the maximum flattening of pin-by-pin power distribution. When uranium fuel is replaced by MOX one provided that the reactivity due to fuel assemblies is kept constant, the fuel enrichment slightly decreases. However, the average neutron spectrum fission microscopic cross-section for ^{239}Pu is approximately twice that for ^{235}U . Therefore power peaks occur in the peripheral fuel assemblies containing MOX fuel which are aggravated by the interassembly water. Physical zoning has to be applied to flatten the power peaks in fuel assemblies containing MOX fuel. Moreover, physical zoning cannot be confined to one row of fuel elements as is the case with a uniform lattice of uranium fuel assemblies.

Both the water gap and the jump in neutron absorption macroscopic cross-sections which occurs at the interface of fuel assemblies with different fuels make the problem of calculating space-energy neutron flux distribution more complicated since it increases nondiffusibility effects. To solve this problem it is necessary to update the current codes, to develop new codes and to verify all the codes including nuclear-physical constants libraries employed. In so doing it is important to develop and validate codes of different levels - from design codes to benchmark ones.

This paper presents the results of the burnup calculation for a multiassembly structure, consisting of MOX fuel assemblies surrounded by uranium dioxide fuel assemblies. The structure concerned can be assumed to model a fuel assembly lattice symmetry element of the VVER-1000 type reactor in which 1/4 of all fuel assemblies contains MOX fuel.

Two variants are considered which differ in zoning fuel assemblies with MOX fuel:

- no zoning (Variant 13 according to the Russian-American benchmark numbering);
- zoning in two peripheral rows of MOX fuel elements (Variant 14).

The calculations were performed by using the MCU-B /1, 2, 3, 4/, CONSYST-KENO-MAYAK-ORIGEN, TVS-M /5/, HELIOS /6, 7/ and TRIANG-PWR codes.

The MCU-B code belong to the class of benchmark codes since it is based on the Monte Carlo method to calculate neutron fluxes as well as on detailed libraries of microscopic cross-sections for neutron interactions with nuclei. Pin-by pin power distribution calculations with using this code were carried out at zero burnup only.

The code system CONSYST-KENO-MAYAK-ORIGEN (CONKEMO) was used for burnup calculations. This system is also benchmark code since it is based on the Monte Carlo method to calculate neutron fluxes, multigroup constant library and on detailed description of the isotopic composition evolution when burning.

The TVS-M code makes use of a multigroup diffusion approximation taking account of kinetic effects in preparing macroconstants. It is proposed that it will be the main tool for macroconstant preparing for the VVER type reactors (including those with MOX fuel) for the burnup process to calculate power distributions both for fuel assemblies and fuel pins. The main objective of the present paper is to prepare verification data for the validation of this calculation code as applied to reactors using MOX fuel.

The HELIOS code makes use of the collision probability method with current coupling at the boundaries of space elements to solve the neutron transport equation.

The TRIANG-PWR code is based on a few-group diffusion approximation and is principally designed to calculate the burnup in the reactor for assembly-by-assembly power distribution calculations. Macroconstants as a function of burnup are produced by means of the WIMS-D4 /8/ code updated at the SSC RF - IPPE. The present work makes use of this code to develop a simplified model for reactor pin-by-pin power distribution calculation.

Calculations using the MCU-B and TVS-M codes were performed at the RSC "Kurchatov Institute". Calculations using the CONKEMO and TRIANG-PWR codes were performed at the SSC RF - IPPE, those using the HELIOS code were conducted by American side at ORNL.

1. SPECIFICATION OF CALCULATIONAL BENCHMARKS

1.1. Material Specification

Table 1.1

Material description

Material	Comment	Isotopic content, 10^{-24} cm^{-3}			
FU1	Fresh uranium fuel	²³⁵ U	$8.7370 \cdot 10^{-4}$	¹⁶ O	$3.9235 \cdot 10^{-2}$
		²³⁸ U	$1.8744 \cdot 10^{-2}$		
FU2	Fresh MOX fuel	²³⁵ U	$3.8393 \cdot 10^{-5}$	²³⁹ Pu	$6.5875 \cdot 10^{-4}$
		²³⁸ U	$1.8917 \cdot 10^{-2}$	²⁴⁰ Pu	$4.2323 \cdot 10^{-5}$
		¹⁶ O	$4.1707 \cdot 10^{-2}$	²⁴¹ Pu	$7.0246 \cdot 10^{-6}$
FU12	MOX fuel of type 1 in zoned FA	²³⁵ U	$3.7918 \cdot 10^{-5}$	²³⁹ Pu	$8.7697 \cdot 10^{-4}$
		²³⁸ U	$1.8683 \cdot 10^{-2}$	²⁴⁰ Pu	$5.6343 \cdot 10^{-5}$
		¹⁶ O	$4.1707 \cdot 10^{-2}$	²⁴¹ Pu	$9.3516 \cdot 10^{-6}$
FU13	MOX fuel of type 2 in zoned FA	²³⁵ U	$3.8786 \cdot 10^{-5}$	²³⁹ Pu	$4.7835 \cdot 10^{-4}$
		²³⁸ U	$1.9111 \cdot 10^{-2}$	²⁴⁰ Pu	$3.0733 \cdot 10^{-5}$
		¹⁶ O	$4.1707 \cdot 10^{-2}$	²⁴¹ Pu	$5.1009 \cdot 10^{-6}$
FU14	MOX fuel of type 3 in zoned FA	²³⁵ U	$3.8959 \cdot 10^{-5}$	²³⁹ Pu	$3.9862 \cdot 10^{-4}$
		²³⁸ U	$1.9196 \cdot 10^{-2}$	²⁴⁰ Pu	$2.5610 \cdot 10^{-5}$
		¹⁶ O	$4.1707 \cdot 10^{-2}$	²⁴¹ Pu	$4.2507 \cdot 10^{-6}$
CL1	Cladding	Zr	$4.230 \cdot 10^{-2}$		
MOD1	Hot moderator with 0.6 g/kg of natural boron	H	0.04783	¹⁰ B	$4.7344 \cdot 10^{-6}$
		¹⁶ O	0.02391	¹¹ B	$1.9177 \cdot 10^{-5}$
MOD3	Cold moderator with 0.6 g/kg of natural boron	H	0.06694	¹⁰ B	$6.6262 \cdot 10^{-6}$
		¹⁶ O	0.03347	¹¹ B	$2.6839 \cdot 10^{-5}$

1.2. Geometry Description

There are three types of geometric objects:

- a three-zone elementary cell (*C3*);
- an assembly containing 331 elementary cells of three types (*K331*);
- a multi-assembly structure formed by assemblies of two types (*MK2*).

A three-zone elementary cell C3 is :

1-st zone - $\text{Cyl}(r_0, r_1 = 0.386 \text{ cm})$;

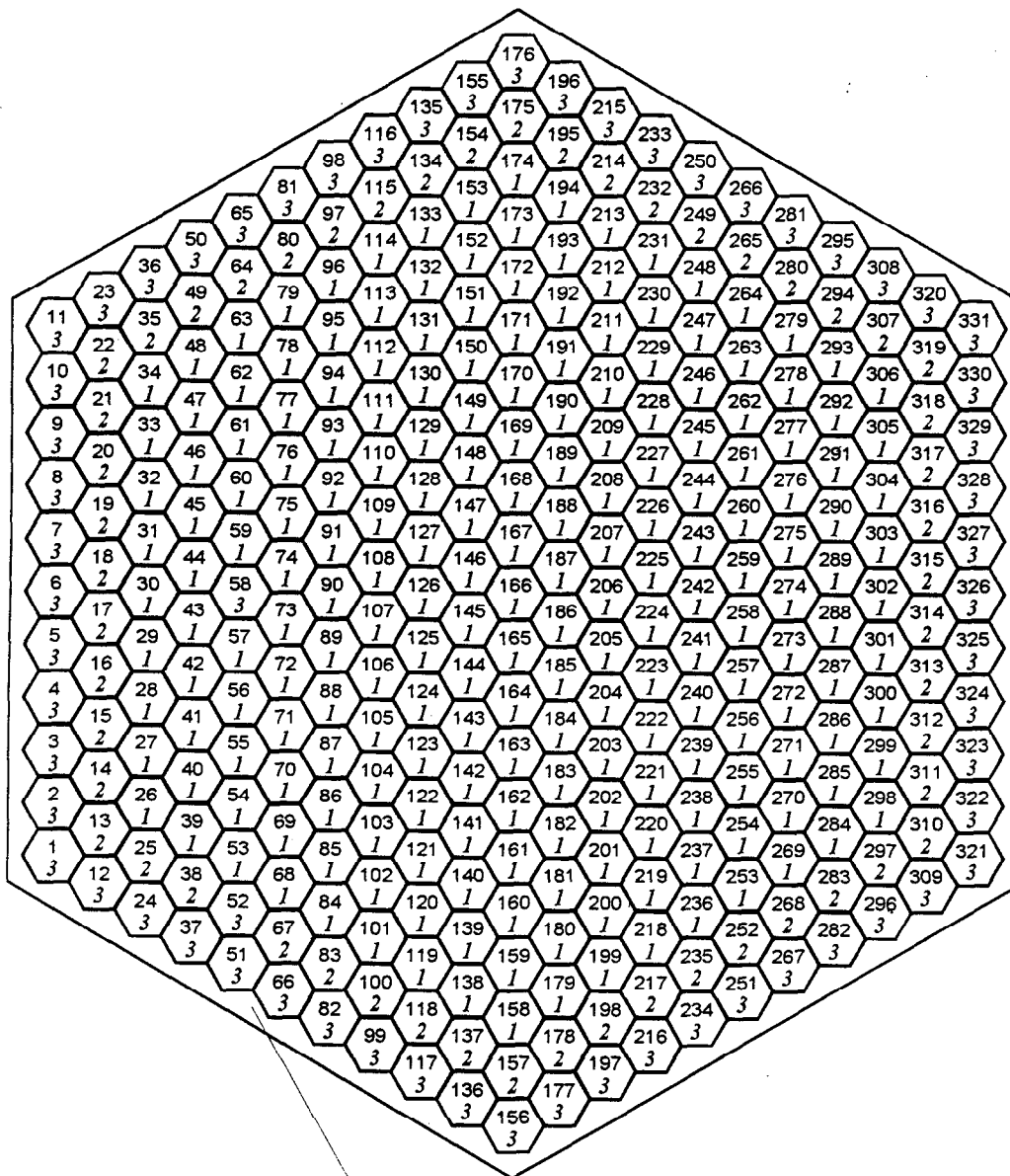
2-nd zone - $\text{Cyl}(r_0, r_2 = 0.4582 \text{ cm}) \setminus \text{Cyl}(r_0, r_1)$;

3-d zone - $\text{Hex}(r_0, h = 1.275 \text{ cm}) \setminus \text{Cyl}(r_0, r_2)$;

were $\text{Cyl}(r_0, r_j)$ is a cylinder of radius r_j with the center at point r_0 ;
 $\text{Hex}(r_0, h = 1.275 \text{ cm})$ is a hexagon with the center at point r_0 and
 across flats dimension $h = 1.275 \text{ cm}$.

Assembly K331 :

This structure is a "container" $\text{Hex}(r_0, H = 23.6 \text{ cm})$, that contains 331 elementary cells *C3* of three types (see Fig. 1.1).



1 - cell number
2 - cell type

"Container" zone

Fig. 1.1. Assembly K331

Multi-assembly structure MK2:

It is formed by an unlimited number of *K331* assemblies of two different types (see Fig. 1.2):

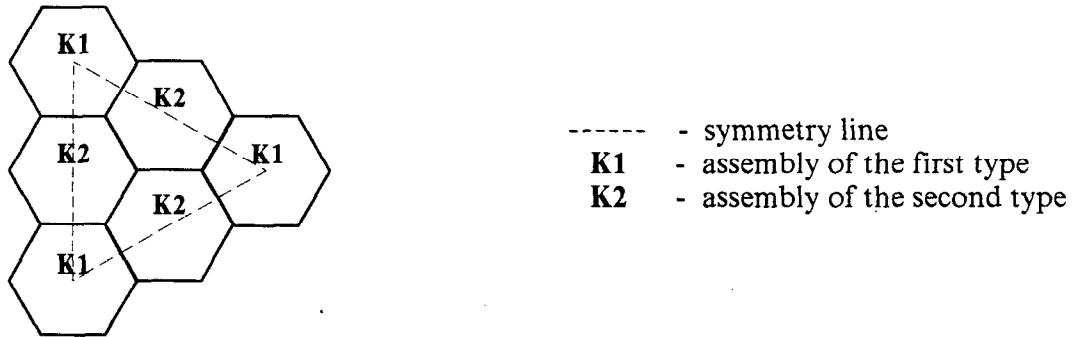


Fig. 1.2. Multi-assembly structure MK2

1.3. A Set of States to Be Calculated

Calculations of multi-assembly structure neutronic parameters should be performed for two states which differ from each other by moderator and fuel temperatures and so on. The state parameters are given in Table 1.2.

Table 1.2

State parameters

State	Temperature of fuel zones, K	Temperature of non-fuel zones, K	Moderator material	¹³⁵ Xe, ¹⁴⁹ Sm	B _z ² , cm ⁻²
S1	1027	579	MOD1	≠ 0. (*)	0.003(**)
S6	300	300	MOD3	0.	0.003(**)

(*) - $\rho(^{135}\text{Xe})=9.4581\text{E-}9$, $\rho(^{149}\text{Sm})=7.3667\text{E-}8$ at zero burnup, equilibrium concentrations at nonzero burnup;

(**) - B_z² values given are set for Variant 13, B_z² values for both of states of Variant 14 are taken equal to zero.

Burnup calculation (with specific power 108 MW/m³) should be performed for the state S1 only. The nuclide concentrations obtained in this state should be used for state S6 calculation (except ¹³⁵Xe and ¹⁴⁹Sm concentrations, which are equal to zero in state S6).

All calculations should be performed with zero current boundary conditions.

1.4. Parameters to Be Calculated

The following parameters should be calculated as a function of burnup (burnup step 2 MWd/kgU) for *state S1*:

- a) K_{eff} ;
- b) K_0 (the ratio of production rate to absorption rate);
- c) pin-by-pin power distribution at 0, 10, 20, 30, 40, 50, 60 MWd/kgU.

1.5. Description of Calculational Variants

Table 1.3

Description of Calculational Variants

Variant number	Comment	Geometry type	Assembly type	Cell type	Zone number	Zone material	Maximum burnup
V13	Multi-assembly structure with nonzoned MOX FA	MK2	1 - K331	1	1	FU2	60.
					2	CL1	
					3	MOD(*)	
				2	1	FU2	
					2	CL1	
					3	MOD(*)	
			2 - K331	1	1	FU1	
					2	CL1	
					3	MOD(*)	
3	1	1	FU1				
		2	CL1				
		3	MOD(*)				

Table 1.3 (continue)

Variant number	Comment	Geometry type	Assembly type	Cell type	Zone number	Zone material	Maximum burnup
V14	Multi-assembly structure with zoned MOX FA	MK2	1 - K331	1	1	FU12	60.
					2	CL1	
					3	MOD(*)	
				2	1	FU13	
					2	CL1	
					3	MOD(*)	
			3	1	FU14		
				2	CL1		
				3	MOD(*)		
2 - K331	1	1	FU1				
		2	CL1				
		3	MOD(*)				
	2	1	FU1				
		2	CL1				
		3	MOD(*)				
3	1	FU1					
	2	CL1					
	3	MOD(*)					

$$(*) \text{ MOD} = \begin{cases} \text{MOD1, } S = S1 \\ \text{MOD3, } S = S6 \end{cases}$$

2. BRIEF DESCRIPTION OF CALCULATIONAL CODES

2.1. MCU-B Code

The MCU-B code with constant library DLC/MCUDAT-2.1 /1/ and BURNUP module /2/ has been developed to predict isotopic composition of the burnable materials of the VVER type reactor depending on its lifetime. The following parameters of the burnable materials are taken into account during calculation:

- change of average cross sections depending on time;
- change of initially present isotope concentration and occurrence of new stable and radioactive nuclides.

Multiplication factor, other neutronic reactor characteristics are obtained simultaneously with isotopic composition calculation.

Thus, MCU-B enables to predict multiplying performance of the reactor and burnable material isotopic compositions depending on operating time and load schedule.

The MCU-B code is developed on the basis of the MCU-RFFI/A code /3, 4/.

Module BURNUP is used for the calculation of the isotopic composition at time step with the given cross-sections of the nuclides and specific power.

MCU-B code burnable materials map using for burnup calculations of the V13 and V14 Variants is shown on Fig. 2.1.

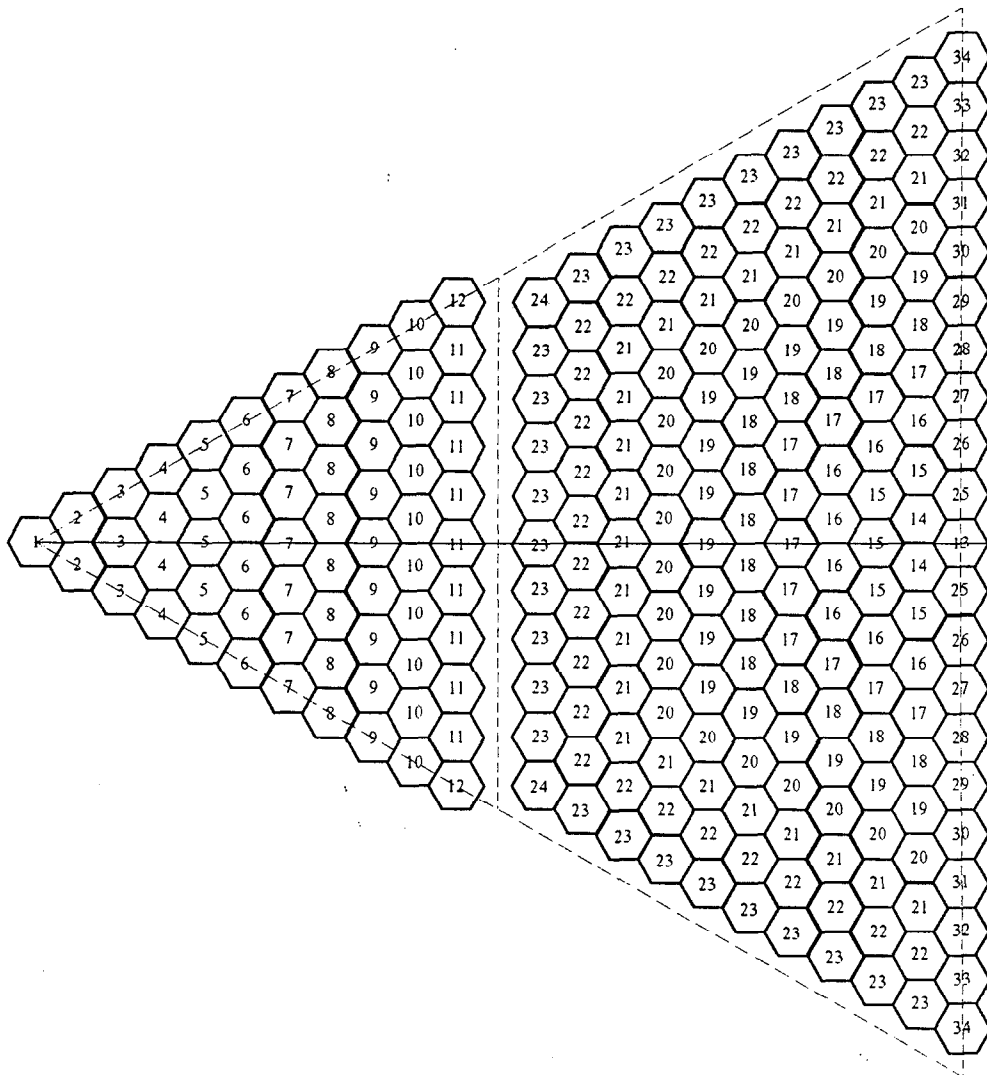


Fig. 2.1. MCU-B code burnable material map for burnup calculations of V13S1 and V14S1 Variants

2.2. Program-Constant Complex CONSYST-KENO-MAYAK-ORIGEN

Code complex CONKEMO was specially developed for burnup calculations. Its diagram is shown on Fig. 2.2. The parts of the complex used for calculations of Variants 13, 14 are marked with the bold line.

- CONSYST prepares the group (299 groups) cross-sections of medium based on ABBN-93 neutron data library /9/;
- KENO-VI is used for neutronic flux calculations in an arbitrary geometry (including hexagonal one) by the Monte Carlo method;
- ORIGEN performs isotope evaluation calculations;
- MAYAK provides the joint work of the codes in the complex, information flows, process the results.

Short descriptions of the above mentioned codes are given below.

The CONSYST code is the main part of CONSYST2 cross-section provision system which provides the use of ABBN-93 cross sections for different practical applications. CONSYST calculates microscopic group cross-sections of nuclides in the medium, neutron and photon cross-sections of the medium etc. CONSYST provides cross-sections for such transport codes as ANISN, DOT, TWODANT, also it gives an opportunity to make use of ABBN-93 data in KENO-VI Monte Carlo calculations etc. CONSYST2 system also includes sets of service procedures. For example, there is a set of procedures which read data from GMF file - the output file of CONSYST. These data are further used in MAYAK code.

KENO-VI / 10/ is a part of American SCALE4.3 system and performs precision calculations in arbitrary three-dimensional geometry by the Monte Carlo method.

ORIGEN-S /11/ (further ORIGEN) is also a part of the SCALE4.3 system. Cross-sections from original ORIGEN libraries are updated during the calculations. The description of this process is below in the text.

MAYAK makes possible the joint use of CONSYST processing code together with neutron and photon transport codes (TWODANT, KENO, and MCNP) with burnup codes (ORIGEN or CARE /12/). Set of batch files provides sequential code start up.

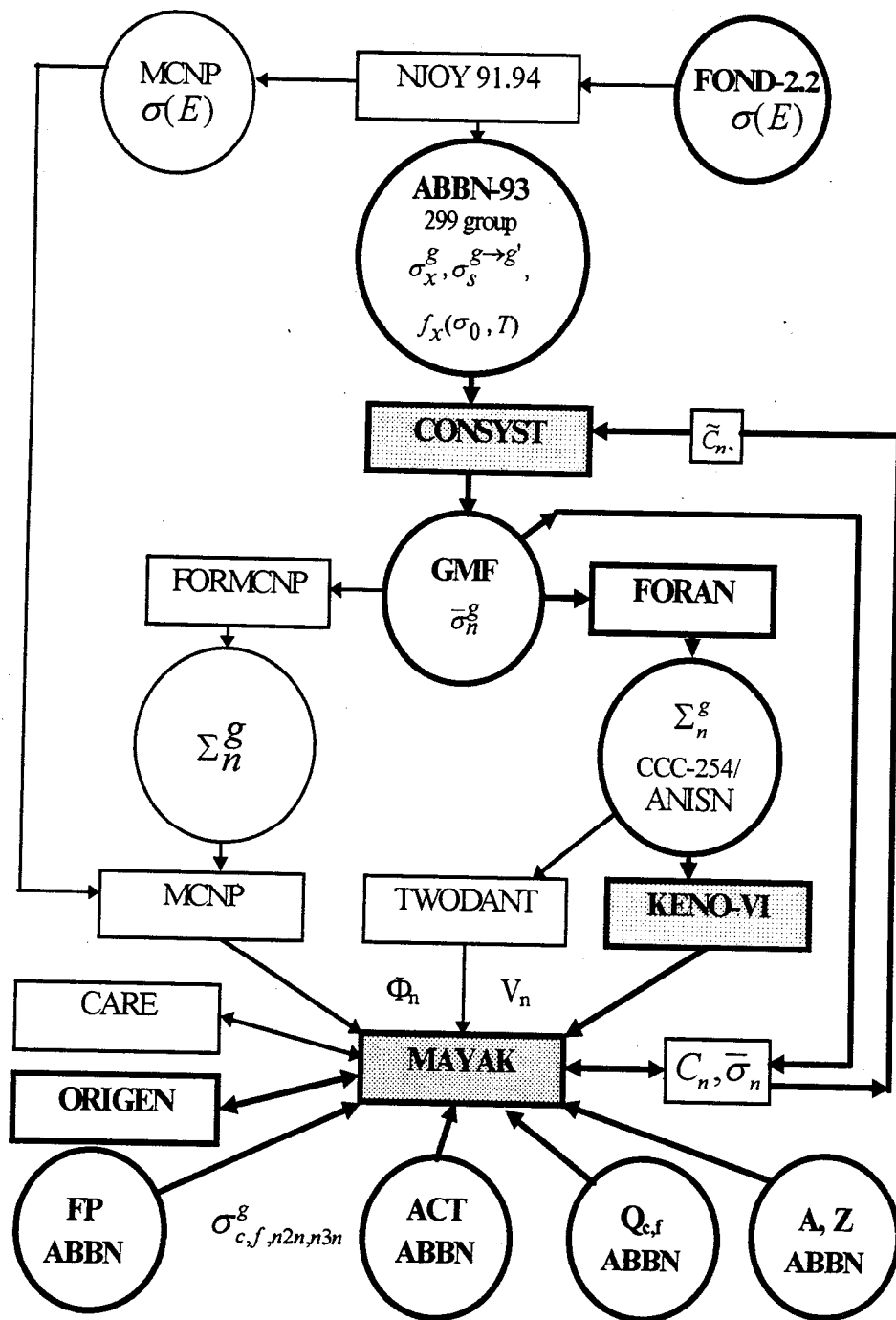


Fig. 2.2. Block diagram of program-constant complex

CONSYST starts first, going through the following steps : 1) reading the input feed data, 2) reading data from ABBN-93 neutron and photon libraries, 3) calculating self-shielding factors for all nuclides in all zones in energy groups specified (in this case 299 groups). If required, the heterogeneity can be considered, 4) writing to Generalized Microconstants File (GMF) the calculation results - microscopic cross-sections of nuclides $\bar{\sigma}_n^g$ for each zone n, 5) compiling the files of medium macro cross-sections Σ_n^g (cross-sections for isotopes or their mixtures) in CCC-254/ANISN format, which is used by transport codes for neutron and photon flux calculations in P_n -approximations of scattering kernel.

The transport code runs then with the cross-sections prepared by CONSYST. It is the KENO-VI code for the case described.

MAYAK receives information about averaged fluxes and the geometry of the computational model from a transport code. CONSYST provides MAYAK with isotopic and microscopic cross-sections. Some external libraries are also used. MAYAK performs the normalization of fluxes per power of the system, formats the information for the burnup code and provides the interaction of different parts of the program complex. MAYAK also calculates some additional values such as weighted cross sections, reaction rates, others, and writes these values to external files.

The cross-section processing, transport, depletion, and MAYAK codes are driven by a system of batch files that provide the possibility of multistep burnup calculations.

The ORIGEN code starts next. A special EXCHANGE format is used for the information exchanges between MAYAK and burnup codes. The format allows to deliver all the information needed to produce the input feed for ORIGEN (concentrations C_n , one-group cross-sections $\bar{\sigma}_n$, neutron fluxes, power, radiation history) as well as take back the new concentrations and cumulative fission product capture cross-section.

While the input for ORIGEN is being created the neutron cross-sections are updated in the ORIGEN libraries. The cross-sections blockings from CONSYST is being taking into account and for the absent isotopes required for calculations of burnup chains cross-sections are read from external neutron group libraries ABBN. These libraries are: a) FP-fission products and b) ACT - neutron cross-sections for actinides. The library of atomic masses is also used.

Multigroup (299 groups) library of fission products contains only radiation capture cross-sections (as original ORIGEN library). These cross-sections are produced on the base of the FOND2.2 library of evaluated neutron files for 169 nuclides.

When ORIGEN stops MAYAK updates the input file for CONSYST for next calculated step with concentrations in zones after burnup process. So calculated cycle is closed.

2.3. Description of Methodical Basis of the TVS-M Code

TVS-M is the spectral code for calculations of neutronic constants of cells, supercells, and fuel assemblies of VVER reactors. It is a component of the code package for VVER calculations.

A constants library used by TVS-M is based on almost the same nuclear data as the MCU-RFFI/A code and has the following main features:

- In the fast energy region ($E_n > 4.65$ keV), the multigroup cross-sections library ABBN is applied. This energy range includes 12 groups of the library. In parallel with the nuclides group constants, the subgroup ones are used.

The subgroup method allows one to express in a simplified form the average of any function g of, say, the total cross-section σ_t , which is given by

$$\langle g \rangle = \int_{\sigma_{tL}}^{\sigma_{tU}} g(\sigma_t) \cdot P(\sigma_t) d\sigma_t,$$

where σ_{tL} and σ_{tU} - are the lower and upper limits of the σ_t variation in an energy interval ΔE ;

$P(\sigma_t)$ - is the probability that the total cross-section has a value σ_t in that interval /13/.

- The resonance energy range ($4.65 \text{ keV} > E_n > 0.625 \text{ eV}$) includes the ABBN groups from 13th to 24th (the cross-sections of the 24th group are modified because the lower boundary of this group is not coincident with the one of the ABBN library). In this energy range the TVS-M code also uses both subgroup and group constants. Besides, the files of resonance parameters from the LIPAR-3 library are applied for resonance nuclides. For most of these nuclides, the cross-section calculation is based on the Breit-Wigner multilevel model (and on the Adler-Adler model for fissile nuclides).
- The thermal energy range ($E_n < 0.625 \text{ eV}$) is subdivided into 24 groups. A set of scattering matrices calculated for various temperatures by the Koppel-Young model is applied for hydrogen bonded in a water molecule. Group cross-sections of nuclides

and the scattering matrixes have been obtained with the use of the same algorithms and nuclear data (TEPCON library) as in the case of the MCU-RFFI/A code.

- Ninety-six FPs are taken into account under burnup calculation. The TVS-M code uses a library of their yields based on ENDF/B-VI data and group cross-sections from the MCU data library.

The TVS-M calculation technique consists of the following main stages: (1) a detailed calculation of all cell types forming a fuel assembly (such as fuel cell, absorber cell, and so on) is performed, and corresponding sets of few-group constants are computed (number of the groups is arbitrary); then (2) these group-effective constants are used in a group nodal diffusion calculation of the whole assembly.

Computing of the neutron's spatial distribution in the specified energy group structure (or at a specified energy point) is performed by method of passing through probability (similar to the first collision probability method). At the present time, an angular distribution of the one-direction neutron's current at a given zone boundary is described by six angular harmonics. A neutron's reflection at a cell boundary takes into account a real hexagonal form of the boundary. For a calculation of an effective diffusion coefficient, both isotropic and anisotropic probabilities in R and Z directions are computed in the same manner.

In the fast energy region, a detailed calculation is carried out with the use of group and subgroup microscopic cross-sections from the ABBN library. In doing so, each energy group is subdivided into an arbitrary number of intervals of uniform width. The energy loss of a neutron on nonelastic slowing down is described by a continuous function specified by the group matrix of nonelastic transfers. The neutron energy loss on elastic slowing down is also described continuously, taken into account scattering anisotropy in a system of inertia centers. In the resonance region, the slowing down of neutrons is calculated in the same manner as in the fast energy region. Cross-sections of resonance nuclides at each energy point are calculated with the CROSS code using the file of resonance parameters for each nuclide. Interference between potential and resonance scattering, the cross-section's temperature dependence, and *p*-wave contribution into scattering cross-sections are strictly taken into consideration. An effect of mutual overlapping of different resonance nuclides is also taken into account.

A calculation technique applied in the thermal energy region is traditional. The group thermalization equation is solved by the method of passing through probability. The sources are shaped when the upper energy groups are calculated, with Nelkine asymptotic limit of scattering applied for hydrogen.

A nodal diffusion approach with asymptotic and transient trial functions (both for flux and current) is applied for pin-by-pin calculation of the fuel assembly. The asymptotic solution corresponds to the problem with a nonzero source (slowing down or fission) and zero current at the cell boundary. The transient trial function corresponds to the problem of finding the neutron distribution in the cell placed at the center a supercell when a source in it is equal to zero. And in such a supercell, a fuel cell is surrounded by the water and a cell of the other type - by homogenized fuel cells. A correction for mesh width is also involved in the balance equation. This correction takes into account the difference between an average flux and a flux at the cell boundary. The similar correction for a current flowing through the cell also appears in the balance equation.

The burnup equations are solved for every fuel pin, which can be subdivided into several concentric rings forming separate burnup zones. Concentration changing of the following heavy nuclides is taken into consideration:

^{232}Th	^{233}Pa	^{233}U	^{234}U	^{235}U	^{236}U	^{238}U	^{237}Np	^{238}Pu	^{239}Np
^{239}Pu	^{240}Pu	^{241}Pu	^{242}Pu	^{241}Am	$^{242\text{m}}\text{Am}$	^{243}Am	^{242}Cm	^{243}Cm	^{244}Cm

Equilibrium concentrations of ^{135}Xe and ^{149}Sm are also calculated.

Calculation of the accumulation of the following 96 FPs is performed for each fuel pin:

^{82}Kr	^{83}Kr	^{84}Kr	^{85}Kr	^{85}Rb	^{86}Sr	^{86}Kr	^{87}Kr	^{87}Rb	^{88}Sr
^{89}Y	^{90}Sr	^{90}Zr	^{91}Zr	^{92}Zr	^{93}Zr	^{94}Zr	^{95}Mo	^{96}Zr	^{96}Mo
^{97}Mo	^{98}Mo	^{99}Tc	^{100}Mo	^{100}Ru	^{101}Ru	^{102}Ru	^{103}Rh	^{104}Ru	^{104}Pd
^{105}Pd	^{106}Pd	^{106}Ru	^{107}Pd	^{108}Pd	^{109}Ag	^{110}Cd	^{111}Cd	^{113}Cd	^{114}Cd
^{115}In	^{116}Sn	^{117}Sn	^{123}Te	^{124}Sn	^{124}Te	^{125}Sb	^{125}Te	^{126}Te	^{127}I
^{128}Xe	^{128}Te	^{129}I	^{129}Xe	^{130}Te	^{130}Xe	^{131}Xe	^{132}Xe	^{133}Cs	^{134}Cs
^{134}Xe	^{135}Cs	^{136}Ba	^{136}Xe	^{137}Cs	^{137}Ba	^{138}Ba	^{139}La	^{140}Ce	^{141}Pr
^{142}Ce	^{142}Nd	^{143}Nd	^{144}Ce	^{144}Nd	^{145}Nd	^{146}Nd	^{147}Pm	^{148}Nd	^{148}Sm
^{149}Sm	^{150}Nd	^{150}Sm	^{151}Sm	^{152}Sm	^{153}Eu	^{154}Sm	^{154}Eu	^{155}Eu	^{156}Gd
^{157}Gd	^{159}Tb	^{160}Dy	^{161}Dy	^{162}Dy	^{163}Dy				

2.4. HELIOS Code

HELIOS is a commercial lattice code that is used for the analysis of fuel assemblies and the generations of collapsed cross-sections for full-core analysis codes. The code uses the collision probability method with current coupling for the transport solution. The subgroup method is used for resonance treatment. A detailed set of nuclides is used for the fuel depletion. Cross-sections based on ENDF/B-VI are available in 34-, 89-, and 190-group libraries. The reference cross-section library used in this work is the 190-group library.

2.5. Program Complex TRIANG-PWR

The program complex TRIANG-PWR is a new version of TRIANG code /14/ for three-dimensional calculations of VVER reactors. TRIANG-PWR is used for simulation of (1) reactor burnup while maintaining criticality by adjusting the concentration of dissolved boron in the coolant and (2) refuelling.

Three-dimensional neutron fluxes are calculated by the diffusion approximation.

Number of points in a plane is 6000 (base variant). Angles of a symmetry from 30° to 180° on a triangular (in a plane) grid are accepted. The maximum number of planes is 50.

TRIANG-PWR is used mainly for three-dimensional, rough mesh calculations of VVER type reactors. A grid with 7 nodes per one fuel assembly is usually used. If needed, more detailed geometric descriptions with tighter grids are possible. In this case the specific cells containing, for example, absorber regions (absorber/burnable absorber rods surrounded by fuel pins) are formed within the assembly. A grid pitch will be something like the trebled fuel pin one. Fine mesh (pin-by-pin) calculations are possible too.

To save computation time, the few-group approach is utilized. The homogenized macroscopic cross-sections of zones of a three-dimensional model are determined from cell (fuel assembly) calculations. The macroconstants, generally speaking, depend on instantaneous conditions of fuel assembly operation: water density, temperature of water and fuel, concentration of a dissolved boron, etc.

To obtain accurate macroscopic cross-sections, an iterative process is required. In a complex TRIANG mode, the correction of constants can be produced through a given number of external iterations.

The WIMS-ABBN code is used to make cell burnup calculations and, as a result, to obtain few-group macroscopic cross-sections. Then the program PARSEC determines approximating coefficients as a function of state variables for zone required. These coefficients are used by the TRIANG code to calculate and to correct macroscopic cross-sections during reactor calculations.

In present work the TRIANG code was used for pin-by-pin calculations of multi-assembly structure (Variants V13 and V14). All cell macroconstants during burnup were found in according with benchmark specification at constant water density and temperature, fuel temperature and dissolved boron concentration.

2.6. WIMS-ABBN

The WIMS-ABBN code is an updated, English WIMS-D4 code /8/. The modernization mainly was done to introduce minor actinide chains and to update the library /15/. Data for almost all structural materials, all neutron moderators, and all actinides were updated in the WIMS-D4 library. Data for Sn, Mo, Hf, Ta, and W were added. Data for minor actinides ^{237}Np , ^{238}Pu , ^{241}Am , ^{242}Am , $^{242\text{m}}\text{Am}$, ^{243}Am , ^{242}Cm , ^{243}Cm , ^{244}Cm , and ^{245}Cm were also added.

The FP list was preserved as in the original version, but all the neutron data for FPs were updated and replenished. Now, full neutron constant sets are included in the library, not simply the capture cross-sections as in earlier versions of the library. The FP yields are updated for ^{235}U and ^{239}Pu , and the yields for all other fissile materials are added.

Group constants for the new WIMS-D4 library were calculated on the basis of the FOND-2 evaluated neutron data library. In many cases, the evaluated nuclear data libraries of ENDF/B-6 and JEF-2 are also used.

Resonance self-shielding data were calculated using the GRUCON code but only in the cases when the narrow resonance approximation may be considered as adequate. The NJOY code was used for calculation of resonance self-shielding, taken into account the fluctuations of collision density in the vicinities of resonance. The NJOY calculations were performed for ^{232}Th , ^{233}U , ^{234}U , ^{235}U , ^{236}U , ^{238}U , ^{239}Pu , ^{240}Pu , ^{242}Pu , ^{241}Am .

Thermalization matrices for moderators were calculated on the basis of ENDF/B-6 data by the NJOY code. Anisotropy of scattering is described in P_1 approximation.

Average group cross-section and matrices of intergroup transitions were calculated using the NJOY code.

In WIMS calculations, a set of 48 nuclides, consisting of 16 actinides, 31 FPs, and oxygen, were used to represent fuel composition and are listed in Table 2.2. The additional neutron reaction cross-section library ACTWIMS is compiled. This library includes the data for many more nuclides and reaction types than does the main WIMS-D4 library. But energy grids in these libraries are the same, and thus the ACTWIMS data can be collapsed using the neutron spectra calculated by WIMS. Collapsed one-group constants can be further used as an input data for any isotope kinetics code.

Table 2.2

Nuclides representing fuel composition

Actinides							
²³⁴ U	²³⁵ U	²³⁶ U	²³⁸ U	²³⁷ Np	²³⁸ Pu	²³⁹ Pu	²⁴⁰ Pu
²⁴¹ Pu	²⁴² Pu	²⁴¹ Am	²⁴³ Am	²⁴² Cm	²⁴³ Cm	²⁴⁴ Cm	²⁴⁵ Cm
FPs							
⁸³ Kr	⁹⁵ Mo	⁹⁹ Tc	¹⁰¹ Ru	¹⁰³ Ru	¹⁰³ Rh	¹⁰⁵ Rh	¹⁰⁵ Pd
¹⁰⁸ Pd	¹⁰⁹ Ag	¹¹³ Cd	¹¹⁵ In	¹²⁷ I	¹³¹ Xe	¹³³ Cs	¹³⁴ Cs
¹³⁵ Xe	¹⁴³ Nd	¹⁴⁵ Nd	¹⁴⁷ Pm	¹⁴⁷ Sm	¹⁴⁸ Pm	¹⁴⁹ Sm	¹⁵⁰ Sm
¹⁵¹ Sm	¹⁵² Sm	¹⁵³ Eu	¹⁵⁴ Eu	¹⁵⁵ Eu	¹⁵⁷ Gd	Lumped FP	
Oxygen							
¹⁶ O							

Improvements were introduced in WIMS-D4. Resonance self-shielding of neutron cross-sections is extended to the thermal region. This improvement is especially important for the accurate treatment of neutron capture in ²⁴²Pu, which has a resonance at very low energy (2.68 eV). The second improvement consists of the addition of a special module (AVERAGE) for collapsing the ACTWIMS cross-sections using WIMS's cell-averaged neutron spectra. Collapsed one-group cross-sections are then used in kinetics calculations.

The number of nuclear reactions considered in the WIMS library during actinide generation was considerably extended. However, the structure of the WIMS-D4 library does not allow the inclusion of some nuclear reactions. The production of ²⁴²Am and ^{242m}Am by the ²⁴¹Am neutron capture cannot be taken into account today because the current version of the WIMS-D4 code cannot treat branching in the capture process. Thus, the production of ²⁴²Cm, ²⁴³Cm, ²⁴⁴Cm and ²⁴⁵Cm are considered inaccurately. For this reason, for any nuclide, the reaction (n, 2n) cannot be considered if the reaction (n, γ) has been included.

The CREDE code was produced to correct these flaws. This code works together with WIMS and AVERAGE. The CREDE code is used for calculations of heavy metal (HM) ($229 \leq A \leq 245$) and its decay products concentrations during burnup and over a long period after unloading. It should be noted that these refinements, as a rule, are insignificant for the nuclides having effect on neutron balance and their influence on WIMS neutron flux calculations are not taken into account.

Figure 2.3 shows the nuclide chains that are taken into account in the CREDE code depletion calculations.

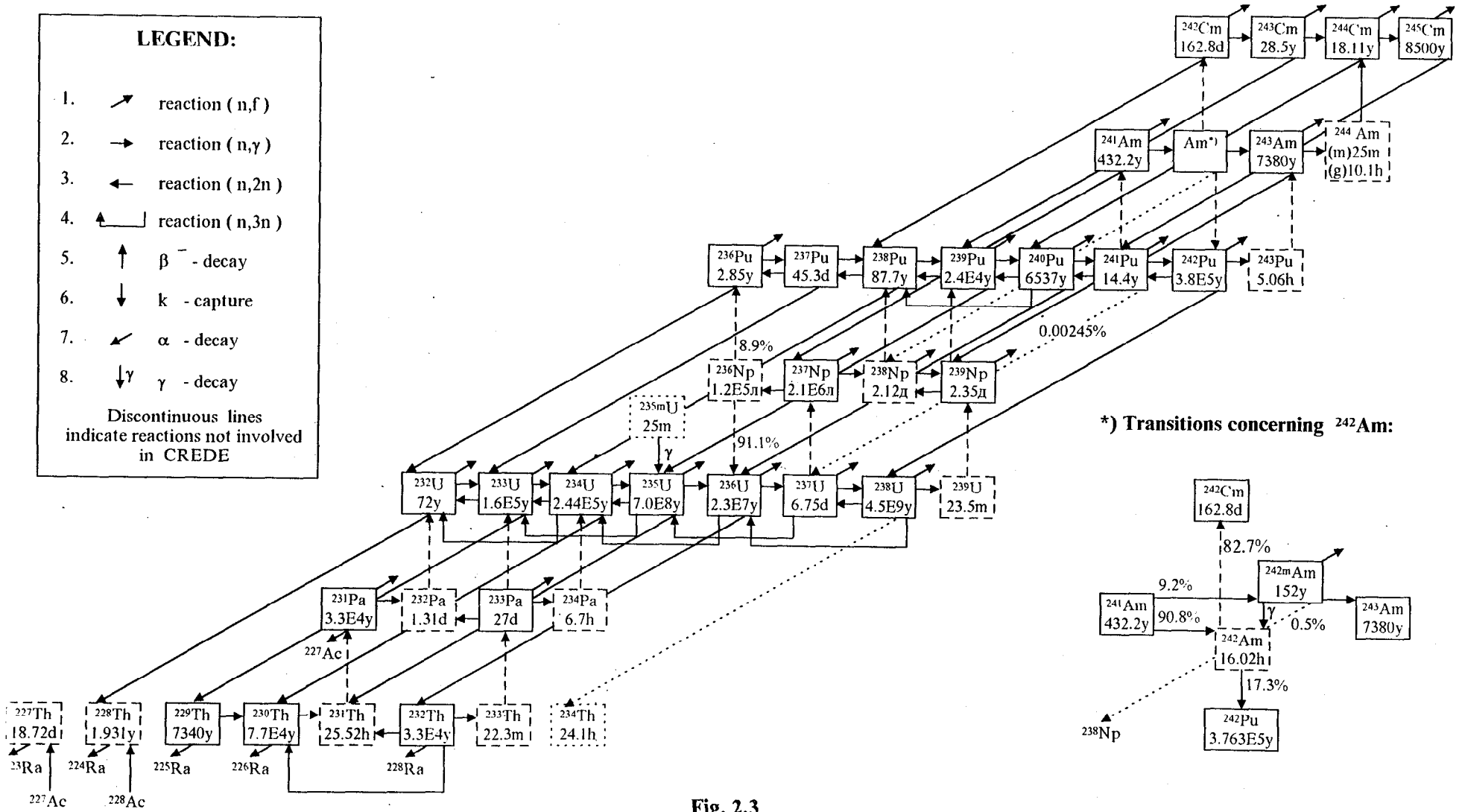
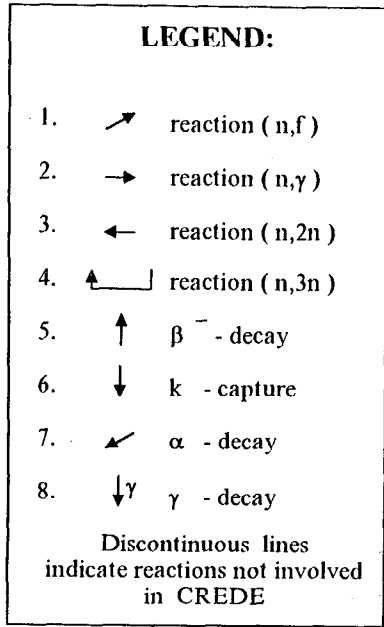


Fig. 2.3

3. CALCULATION RESULTS

A brief description of the methods of the burnup calculation by using the MCU code was given in section 2. As shown in Fig. 2.1, the above calculation considered several different fuel elements as one burnable material. This approximation is unlikely to cause any significant error in calculating the dependence of K_{eff} of the system on the burnup. For significant burnups, however, power distributions thus obtained cannot be considered to be valid enough. Therefore the present paper considers power distributions only for the beginning of the burnup.

By employing the CONKEMO code calculations were performed for each of 127 fuel pins occurring in the symmetry sector (1/12 of the multiassembly structure) to determine changes in the isotopic composition and the neutron flux after each time step. Two sets of calculations were conducted for both variants: one set using the burnup step of 20 MWd/kg, the other using the burnup step of 10 MWd/kg. The Runge-Kutta method of the second order accuracy was applied for Variant 13, that is, neutron fluxes were calculated twice at each step using KENO-VI. To calculate Variant 14 a simple step method was employed, that is, the flux was calculated once at each time step. It should be noted, however, that in both cases the fuel pin power was conserved instead of neutron flux at every calculation step when the ORIGEN burnup calculations in each fuel pin were performed. This approximation enables the burnup calculation step to be increased what is important when the Monte Carlo method is used to calculate the neutron flux.

When employing the TVS-M, HELIOS and TRIANG codes the burnup step was chosen so that its further decrease could not affect the accuracy of the results.

The calculation of neutron fluxes after each burnup step by KENO-VI considered 7×10^6 histories.

The KENO-VI code cannot perform calculations with the buckling other than zero. Therefore, as regards Variant 13, the height of the system was estimated to be equivalent to the buckling value equal to 0.003. This height proved to be 50 cm. This estimate was obtained by the MCU code.

3.1. Comparison of the Calculation Results Obtained by the CONKEMO Code with Different Time Steps

Table 3.1. presents the calculation results of K_{eff} in S1 state obtained by the CONKEMO code with different time steps.

Table 3.1

Dependence of K_{eff} on the burnup
obtained by the CONKEMO code for S1 state with different time steps

Burnup, MWd/kg HM	K_{eff}			
	Variant 13		Variant 14	
	Step 20 MWd/kg	Step 10 MWd/kg	Step 20 MWd/kg	Step 10 MWd/kg
0	1.0554	1.0554	1.2646	1.2646
10		0.9630		1.1553
20	0.8990	0.8950	1.0804	1.0764
30		0.8407		1.0072
40	0.7928	0.7913	0.9517	0.9468
50		0.7488		0.8940
60	0.7120	0.7118	0.8524	0.8483

Table 3.1. shows that in both variants the maximum discrepancy in K_{eff} calculated with different burnup steps does not exceed 0.5%. Variant 13 shows somewhat less significant dependence on the burnup step. This is due to greater accuracy of the Runge-Kutta method employed in calculating this variant compared to the method of simple steps employed for Variant 14. Since the error of the simple steps technique is proportional to step, the maximum error when calculating with step equal to 10 MWd/kg can be estimated as 0.5 % as compared with Variant 14 calculation using infinitely small step. The maximum error in Variant 13 is likely to be less, since the error of the Runge-Kutta method of the second order accuracy is proportional to square of step value.

Figs. 3.1 and 3.3 present pin-by-pin power distributions for the end of burnup for Variants 13 and 14 in state S1, which were obtained using different steps. Figs. 3.2 and 3.4 show relative discrepancies in distributions presented in Figs. 3.1 and 3.3, respectively:

$$\frac{CONKEMO(\Delta t = 20) - CONKEMO(\Delta t = 10)}{CONKEMO(\Delta t = 10)} \cdot 100\%.$$

The same figures present the numbers of the zones in which the fuel pins are assumed to be integrated to perform analysis. The lower part of the figures shows arithmetic mean and root-mean-square deviations in particular zones as well as the number of calculation points in the zones. Maximum distinctions in plutonium and uranium fuel assemblies as well as the coordinates of fuel pins of which these distinctions occur are given too. (See row number from bottom to top, point number from left to right.)

Figures 3.2 and 3.4 show that the maximum discrepancies in power distributions for the end of the burnup obtained with different burnup steps in both Variants are about 3%. Due to the above mentioned linear dependence of the calculation error on the burnup step the maximum calculation error in Variant 14 with the burnup step of 10 MWd/kg, related to the finiteness of the step, can be estimated to be 3% as well. In variant 13 the error is likely to be less due to the root-mean-square dependence on the burnup step.

The values of K_{eff} and power distribution obtained by the CONKEMO code with the step of 10 MWd/kg are presented below to enable them to be compared with the data obtained by other codes.

3.2. Comparison of the K_{eff} Value Calculation Results

Tables 3.2. and 3.3 show dependence of K_{eff} on the burnup calculated in Variants 13 and 14 by the MCU-B, CONKEMO, TVS-M and HELIOS codes. The MCU code calculation involved $1 \cdot 10^6$ histories (the statistical error in K_{eff} is less than 0.1%).

Table 3.2

Dependence of K_{eff} on burnup for V13 obtained by different codes

Burnup, MWd/kg HM	Variant 13							
	MCU		CONKEMO		TVS-M		HELIOS	
	S1	S6	S1	S6	S1	S6	S1	S6
0	1.0645	1.213	1.0554	1.2037	1.0611	1.2135	1.0600	1.2134
10	0.9692	1.115	0.9630		0.9760	1.1260	0.9710	
20	0.8960	1.036	0.8950		0.9091	1.0510	0.9022	
30	0.8373	0.966	0.8407		0.8524	0.9840	0.8453	
40	0.7877	0.904	0.7913		0.8022	0.9226	0.7957	
50	0.7441	0.849	0.7488		0.7579	0.8670	0.7525	
60	0.7064	0.802	0.7118	0.8066	0.7195	0.8181	0.7157	

Table 3.4 presents the reactivity shifts on burning and changing the fuel and moderator temperatures in going from operation state to cold one. Reactivity shifts were calculated with the formula:

$$\rho_{1,2} = \frac{K_2 - K_1}{K_1 \cdot K_2},$$

in so doing Tables 3.2 and 3.3 data were used.

Table 3.3

Dependence of K_{eff} on burnup for V14 obtained by different codes

Burnup, MWd/kg HM	Variant 14							
	MCU		CONKEMO		TVS-M		HELIOS	
	S1	S6	S1	S6	S1	S6	S1	S6
0	1.2645	1.360	1.2646	1.3603	1.2626	1.3598	1.2651	1.3629
10	1.1616	1.255	1.1553		1.1636	1.2607	1.1581	1.2608
20	1.0849	1.167	1.0764		1.0834	1.1763	1.0762	1.1749
30	1.0175	1.087	1.0072		1.0157	1.1015	1.0084	1.0993
40	0.9594	1.017	0.9468		0.9558	1.0329	0.9490	1.0302
50	0.9079	0.956	0.8940		0.9027	0.9707	0.8968	0.9676
60	0.8628	0.902	0.8483	0.9069	0.8565	0.9151	0.8521	0.9131

Table 3.4

Reactivity shifts on burnup and changing the fuel and moderator temperatures from operation state to cold one at the beginning and the end of burnup

Code	MCU	CONKEMO	TVS-M	HELIOS
Variant 13				
ρ_{burnup}	-0.476	-0.457	-0.447	-0.454
$\rho_{h-c(0)}$	0.115	0.117	0.118	0.119
$\rho_{h-c(60)}$	0.169	0.165	-0.168	-
Variant 14				
ρ_{burnup}	-0.368	-0.388	-0.376	-0.383
$\rho_{h-c(0)}$	0.056	0.056	0.057	0.057
$\rho_{h-c(60)}$	0.050	0.076	0.075	0.078

The consideration of results presented in Tables 3.2÷3.4 shows:

1. The K_{eff} values for the beginning of burnup in states S1 and S6 calculated with the use of different codes are in good agreement. Maximum discrepancy does not exceed 0.5 %. The exception are the K_{eff} values calculated using CONKEMO code for Variant 13, which are somewhat less (by 0.4÷0.8 ‰). This is likely because the height corresponding to specified buckling was not enough accurately estimated. For Variant 14 with zero buckling, the K_{eff} values calculated using CONKEMO are in a good agreement with other calculations.

2. Burnup reactivity shift and temperature reactivity shift caused by fuel and coolant temperature change in going from operation state to cold one are in a good agreement as well. Maximum discrepancies of results are 6 % for burnup reactivity shift and 4 % for reactivity related with going from operation state to cold one. Only one exception is the reactivity shift related with reactor cooling at the end of burnup in Variant 14, which was calculated using MCU code. This shift is significantly less than those obtained by use of other codes.

3.3. The Results of Power Distribution Calculations Using Benchmark Codes at the Beginning of Burnup

Figs. 3.5 and 3.7 present power distributions at the beginning of burnup for Variants 13 and 14 at state S1 obtained with use of MCU and CONKEMO codes. Figs. 3.6 and 3.8 show relative distinctions in given distributions:

$$\frac{MCU - CONKEMO}{CONKEMO} \cdot 100\%$$

The same figures give arithmetic mean and root-mean-square deviations in the zones and the number of points. Maximum distinctions in plutonium and uranium fuel assemblies as well as the coordinates of fuel pins of which these distinctions occur are given too. (See row number from bottom to top, point number from left to right.)

Figs. 3.6 and 3.8 show that MCU code values of power of fuel pins at assembly boundaries are slightly greater. The most distinctions are about 3 % and 5 % for MOX fuel assembly and uranium one, respectively. This level of agreement between distributions obtained can be considered as satisfactory. However, it seems likely that the cause of pointed above difference in power in peripheral fuel pins should be found out later on.

3.4. Comparison of the Calculations of Power Distributions on Burning Obtained by the TVS-M, HELIOS and CONKEMO Codes

Figs. 3.9÷3.13 show power distributions for burnups of 0, 10, 20, 30, 40, 50 and 60 MWd/kg obtained in Variant 13 by the TVS-M and CONKEMO codes. The calculation values obtained by the HELIOS code are also presented for the initial state.

Figs. 3.16÷3.22 present the corresponding relative distinctions in the calculation results obtained by the TVS-M (HELIOS) code from those calculated by the CONKEMO code:

$$\frac{\text{Code} - \text{CONKEMO}}{\text{CONKEMO}} \cdot 100\%.$$

Similar information for Variant 14 is presented in Figs. 3.23÷3.36. For this particular Variant the HELIOS calculation results are presented for all the burnup values involved.

From the results presented in Figs. 3.16÷3.22 it can be concluded that in all states during burnup in Variant 13 the maximum discrepancy in the results obtained by the TVS-M and the CONKEMO codes does not exceed 4.2% for MOX fuel assemblies and 2.3% for uranium fuel ones. For Variant 14 similar maximum discrepancies are 3.5% and 4.5%, respectively (see Figs. 3.30÷3.36). This shows that pin-by-pin power distributions calculated by the TVS-M code are in good agreement with those obtained by the benchmark CONKEMO code over the whole burnup process.

Calculations performed by the TVS-M code in Variant 13 reveal a slight increase of fuel pin power in MOX fuel assemblies and a slight decrease in uranium fuel assemblies. In Variant 14 this effect only occurs at the initial stage of the burnup.

Maximum discrepancies in calculations by the HELIOS and CONKEMO codes (see Figs. 3.30÷3.36) are close to similar values for the TVS-M code. The exception is the central fuel pin in MOX fuel assemblies where this discrepancy is slightly greater. As seen from Figs. 3.9 and 3.2 in calculations performed by the HELIOS code the fuel pin power in the central point is higher than that in adjacent points. This effect might result from some error in the procedure for calculating the neutron flux in the central point inherent in the code.

3.5. The Statistical Error Estimate on Power Distribution Calculation by CONKEMO Code

Figs. 3.37 and 3.38 present discrepancy of power distributions in Variants 13 and 14 at the beginning of burnup obtained by the TVS-M and CONKEMO codes. Two discrepancies are given for every calculational points: when power distribution is normalized to the average value over (1) the whole calculated region and (2) each isolated zone. The figures also give arithmetic mean and root-mean-square deviations in the zones for distributions normalized to the whole calculated region (tvso) and to the isolated zone (tvs).

Statistical error using the CONKEMO complex occurs due to the KENO code based on Monte Carlo method for neutron flux calculations. Statistical error is absent in the TVS-M code calculations. Because of this, the discrepancies between the TVS-M and KENO calculations comprise statistical error of the KENO calculations and bias error. A bias error can be reduced by distribution normalization to the own average values over the separated zones. Shift of one distribution in each zone with relation to another one is excluded in so doing. However, the discrepancies related with different space dependences of the distributions within the zones and statistical error still remain. Thus, root-mean-square deviations (tvs) in the zones with rather large points may be considered as upper estimate of statistical error.

The Figs. 3.37 and 3.38 show that in both variants the root-mean-square deviations in the zones (tvs) do not exceed 0.6 %. From the above, it follows that this value is an upper estimate of statistical error in pin-by-pin power distribution using the KENO code calculations with about $7 \cdot 10^6$ histories involved.

Fig. 3.37. Discrepancies. V13. S1. Burnup = 0 MWd/kg

On normalization to mean value:

- over the whole calculated region 1.1
- over the calculated zone .4

1
1.1
.4

1 1 1
.6 .7 .7
-.1 .0 .0

1 1 1 1 1
1.1 .7 .8 .9 .9
.4 .0 .1 .2 .2

1 1 1 1 1 1 1
.7 .6 .9 .7 .3 1.0 1.2
.0 -.1 .2 .0 -.4 .3 .5

7 1 1 1 1 1 1 1 1
-.3 .2 .8 .5 .8 .6 .8 .9 .9
-.9 -.5 .1 -.2 .1 -.1 .1 .2 .2

5 6 7 1 1 1 1 1 1 1
.2 .1 .4 .6 1.0 .5 .6 .7 .6 .5 .8
-.6 -.5 -.2 -.1 .3 -.2 -.1 .0 -.1 -.2 .1

15 10 5 6 7 1 1 1 1 1 1 1 1
-.9 .0 .3 .1 .2 .1 .5 .8 .7 .3 .6 .7 .6
.8 .0 -.5 -.5 -.4 -.6 -.2 .1 .0 -.4 -.1 .0 -.1

17 16 15 10 5 6 7 1 1 1 1 1 1 1 1
-1.8 -2.1 -1.4 .0 .1 .3 .3 .6 .7 .5 .9 .6 .8 .5 .4
.4 .4 .3 .0 -.7 -.3 -.3 -.1 .0 -.2 .2 -.1 .1 -.2 -.3

11 11 17 16 15 10 5 6 7 7 7 7 7 7 7 7 7
-2.0 -2.4 -2.3 -2.6 -1.8 .0 -.3 .0 .6 .7 .8 .6 .9 .5 .9 .9 .8
.4 .0 .0 -.1 -.1 .0 -1.1 -.6 .0 .1 .2 .0 .3 -.1 .3 .3 .3

11 11 11 11 17 16 15 10 5 6 6 6 6 6 6 6 6 6
-2.3 -2.9 -2.4 -2.2 -2.1 -2.6 -1.8 .0 -.1 .6 .8 .7 .9 .8 .7 .9 1.3 .9 .7
.1 -.5 .0 .2 .1 -.1 -.1 .0 -.9 -.1 .1 .0 .3 .2 .0 .3 .7 .3 .1

11 11 11 11 11 11 17 16 15 10 4 5 5 5 5 5 5 5 5 4
-2.1 -2.6 -2.2 -2.4 -2.4 -2.3 -2.6 -2.8 -2.0 .0 1.0 1.5 1.3 1.5 1.2 .7 1.2 .4 1.0 .9 1.1
.3 -.2 .2 .0 .0 .1 -.3 -.3 -.4 .0 .0 .7 .6 .7 .5 -.1 .5 -.3 .3 .2 .0

11 11 11 11 11 11 11 17 16 14 10 10 10 10 10 10 10 10 10 10
-2.6 -2.6 -2.5 -2.2 -2.2 -2.3 -2.5 -2.8 -2.3 -2.4 -1.4 .0 .0 .0 .0 .0 .0 .0 .0 .0 .0
-.2 -.2 -.1 .2 .2 .1 -.1 -.4 .0 .1 .0 .0 .0 .0 .0 .0 .0 .0 .0 .0 .0

maxtvs0: Pu -2.9 3 2 ; U 1.5 2 14 maxtvs : Pu .8 6 1 ; U -1.1 4 7

zon	11	12	13	14	15	16	17	1	2	3	4	5	6	7														
tvs0	-2.4	2.42	.0	.00	.0	.00	-1.4	1.42	-1.6	1.68	-2.5	2.53	-2.3	2.27	.7	.70	.0	.00	.0	.00	1.1	1.06	.7	.95	.6	.73	.6	.64
tvs	.0	.21	.0	.00	.0	.00	.0	.00	.0	.36	.0	.26	.0	.23	.0	.22	.0	.00	.0	.00	.0	.02	.0	.60	.0	.37	.0	.29
sum	14.083		.000	.000	.500	4.500	4.500	4.000	42.250	.000	.000	1.500	13.500	13.5														

3.6. Calculation Results Obtained by the TRIANG-PWR Code

The purpose of calculations by the TRIANG-PWR code is to choose the calculational model of given multiassembly structure for using it in the following pin-by-pin power distribution calculations in reactor. Using the few-groups approach realized now in the TRIANG code, the macroconstant preparation during burnup is needed. As noted in section 2, this preparation is made with the use of the WIMS-ABBN calculations and the following approximation of macroscopic cross-sections as a function of variables that describe the reactor state.

When preparing the constants for pin-by-pin calculation it is important to choose an adequate model of fuel cell or supercell (fuel cell and its surroundings). To do this requires to keep the neutron spectrum in fuel and, hence, the behaviour of nuclide composition during burnup. This problem was working out with the use of the CONKEMO calculation results as the benchmarks. In so doing, the calculational region was divided into zones with the same spectrum for every point. Each zone was modelled by the own supercell.

Table 3.5 presents the calculation results of K_{eff} during burnup for Variants 13 and 14 obtained by the TRIANG as compared with similar results obtained by the CONKEMO complex.

Table 3.5

Dependence of K_{eff} value on the burnup
obtained by the TRIANG and CONKEMO codes at state S1

Burnup, MWd/kg HM	K_{eff}			
	Variant 13		Variant 14	
	TRIANG	CONKEMO	TRIANG	CONKEMO
0	1.0553	1.0554	1.2589	1.2646
10	0.9629	0.9630	1.1529	1.1553
20	0.8951	0.8950	1.0717	1.0764
30	0.8392	0.8407	1.0068	1.0072
40	0.7901	0.7913	0.9499	0.9468
50	0.7473	0.7488	0.8996	0.8940
60	0.7111	0.7118	0.8562	0.8483

It is seen from Table 3.5, that K_{eff} values obtained by the TRIANG-PWR code are in reasonably good agreement with those obtained by the CONKEMO code.

Table 3.6 shows the maximum discrepancies in power distributions obtained by the TRIANG and CONKEMO codes.

Table 3.6

Maximum discrepancies
in pin-by-pin power distributions

Burnup, MWd/kg HM	<i>TRIANG - CONKEMO</i> · 100 %			
	<i>CONKEMO</i>			
	Variant 13		Variant 14	
	MOX	UO ₂	MOX	UO ₂
0	2.9	-2.2	2.8	-1.6
10	4.6	-3.5	3.3	-2.0
20	3.9	-2.0	4.5	-3.7
30	3.7	-2.3	3.6	3.8
40	3.6	-1.9	4.0	4.6
50	2.6	-2.0	2.9	3.6
60	4.1	-2.2	3.1	3.2

Figs. 3.39 and 3.41 demonstrate the calculational power distributions obtained by the TRIANG and CONKEMO codes for Variant 13 at 0 and 60 MWd/kg burnups. Figs. 3.40 and 3.42 present discrepancies in power distributions. Similar information for Variant 14 is given on Figs. 3.43÷3.46.

From the results presented in Table 3.6 it is seen that maximum discrepancy in power distributions calculated with the use of the TRIANG code and the benchmark CONKEMO code in Variants 13 and 14 does not exceed 5 % for all burnup steps. By this is meant that the approximation burnup model used in the WIMS-ABBN and the TRIANG-PWR codes is adequate, and it is possible to use this model for calculation of pin-by-pin power distribution in MOX-fuelled core of VVER reactors.

CONCLUSION

The consideration of calculation results for multi-assembly structures (nonzoned and zoned MOX fuel assemblies surrounded by fuel assemblies with UO₂ fuel) allows us to make the following conclusion:

1. The K_{eff} values at the beginning of burnup at operation and cold states obtained by MCU, CONKEMO, TVS-M and HELIOS codes are in a good agreement. The maximum discrepancies of corresponding values do not exceed 0.5 %.

Burnup reactivity shift and reactivity shift caused by fuel and moderator temperature change from operation state to cold one are in a good agreement as well. Maximum discrepancies of results are 6 % for burnup reactivity shift and 4 % for reactivity related with going from operation state to cold one.

2. Comparison of the calculation results obtained by the benchmark MCU and CONKEMO codes shows that the most distinctions in pin-by-pin power distributions are about 3 % and 5 % for MOX fuel assembly and uranium one, respectively. This level of agreement can be considered as satisfactory.
3. Maximum discrepancies in pin-by-pin power distributions for all burnup steps obtained by TVS-M and CONKEMO codes in variant with nonzoned MOX fuel assembly are 4.2 % in MOX fuel assembly and -2.3 % in uranium fuel assembly. In variant with zoned MOX fuel assembly the similar discrepancies are equal to 3.5 % and -4.5 %, respectively. By this is meant that pin-by-pin power distributions obtained by the TVS-M code and the benchmark CONKEMO code are in a good agreement for all burnup steps.

Maximum discrepancies between calculation results obtained by the HELIOS and the CONKEMO codes agree closely with the similar values obtained by the TVS-M code.

4. Maximum discrepancy in pin-by-pin power distributions calculated with the use of the few-groups diffusion TRIANG code and the benchmark CONKEMO code for both variants considered does not exceed 5 % for all burnup steps. By this is meant that the approximation burnup model used in the WIMS-ABBN and the TRIANG-PWR codes is adequate, and it is possible to use this model for calculation of pin-by-pin power distribution in MOX-fuelled core of VVER reactors.

REFERENCES

1. Л.П. Абагян, А.Е. Глушков, М.С. Юдкевич. Библиотека ядерных данных DLC/MCUDAT-2.1. Отчет РНЦ КИ. Инв. № 32/1-35-398 от 25.08.98.
2. М.С. Юдкевич. Программа BURNUP для расчета изменения изотопного состава реактора в процессе кампании. Отчет РНЦ КИ. Инв. № 32/1-36-398 от 25.08.98.
3. Федеральный надзор России по ядерной и радиационной безопасности. Аттестационный паспорт программного средства: "Программа MCU/RFFI/A с библиотекой констант DLC/MCUDAT-1.0". Регистрационный номер паспорта аттестации 61 от 17.10.96.
4. E.A. Gomin, L.V. Maiorov. "The MCU-RFFI Monte Carlo Code for Reactor Design Applications", Proc. of Int. Conf. on Math. and Comp., Reactor Phys. and Envir. Anal., April 29-May 4 1995, Portland, Oregon, USA, (1995).
5. V.D. Sidorenko et. al. Spectral Code TVS-M for Calculation of Characteristics of Cell, Supercells and Fuel Assemblies of VVER-Type Reactors. 5-th Symposium of the AER, Dobogoko, Hungary, October 15-20, 1995.
6. Eduardo A. Villarino et. al., "HELIOS: Angularly Dependent Collision Probabilities", Nucl. Sci. & Eng., V. 112, pp. 16-31.
7. Juan J. Casal, et. al., "HELIOS: Geometric Capability of New Fuel-Assembly Diagram", Proceedings of the Internationale Topical Meeting on Advances in Mathematics, Computations, and Reactor Physics, April 28-May 2, 1991, Pittsburgh, PA, p. 10.21-1.
8. Askew J.R., Fayers E.J., Kemsell P.B. A General Description of the Lattice Code WIMS; J. Brit. Nucl. Energy Soc., 5, 564(1966).

9. Мантуров Г.Н., Николаев М.Н., Цибуля А.М. "Система групповых констант БНАБ-93. Верификационный отчет № 1. Рекомендованные справочные данные", Москва 1995.
10. D.F. Hollenbach, L.M. Petrie, N.F. Landers. KENO-VI: A General Quadratic Version of the KENO Program. SCALE4.3, Vol. 2.2, Section F17, 1995.
11. O.W. Hermann, R.M. Westfall. ORIGEN-S: SCALE System Module to Calculate Fuel Depletion, Actinide Transmutation, Fission Product Buildup and Decay, and Association Source Terms. SCALE4.3, Vol. 2, Section F7, 1995.
12. Кочетков А.Л. "Программа CARE - расчет изотопной кинетики, радиационный и экологический характер ядерного топлива при его облучении и выдержке". Препринт ФЭИ 2431, 1995.
13. Yigal Ronen, ed., CRC Handbook of Nuclear Reactor Calculations, Volume III, CRC Press, Inc., 1986, p. 278.
14. Воронков А.В. и др. "Программы многомерных расчетов ядерных реакторов." В сб. "Программы и методы физического расчета быстрых реакторов". Димитровград, 1974.
15. M. Nikolaev, A. Tsiboulia, G. Gerdev, E. Rozhikhin, V. Koscheev. Updating, Supplementing and Validation of the WIMS-D4 Group Constant Set. S&T Report, French-Russian Seminar. Obninsk, April 24-25, 1995.

INTERNAL DISTRIBUTION

- | | | | |
|--------|-----------------|--------|--------------------------------|
| 1-5. | B. B. Bevard | 22. | G. E. Michaels |
| 6. | J. J. Carbajo | 23. | B. D. Murphy |
| 7. | E. D. Collins | 24. | D. L. Moses |
| 8. | B. S. Cowell | 25. | C. V. Parks |
| 9. | M. D. DeHart | 26-30. | R. T. Primm, III |
| 10. | F. C. Difilippo | 31. | I. Remec |
| 11-15. | J. C. Gehin | 32. | C. C. Southmayd |
| 16. | S. R. Greene | 33. | B. A. Worley |
| 17. | T. W. Horning | 34. | B. S. Yarborough |
| 18. | D. T. Ingersoll | 35. | G. L. Yoder, Jr. |
| 19. | H. T. Kerr | 36. | Central Research Library |
| 20. | M. A. Kuliasha | 37-38. | ORNL Laboratory Records (OSTI) |
| 21. | G. T. Mays | 39. | ORNL Laboratory Records-RC |

EXTERNAL DISTRIBUTION

40. N. Abdurrahman, College of Engineering, Dept. of Mechanical Engineering, University of Texas, Austin, Texas 78712
41. M. L. Adams, Department of Nuclear Engineering, Texas A&M University, Zachry 129, College Station, TX 77843
42. H. Akkurt, College of Engineering, Dept. of Mechanical Engineering, University of Texas, Austin, Texas 78712
43. D. Alberstein, Los Alamos National Laboratory, MS-E502, P.O. Box 1663, Los Alamos, NM 87545
44. J. Baker, Office of Fissile Materials Disposition, U. S. Department of Energy, MD-3, 1000 Independence Avenue SW, Washington, DC 20585
45. H. R. Canter, Office of Fissile Materials Disposition, U. S. Department of Energy, MD-1/2, 1000 Independence Avenue SW, Washington DC 20585
46. A. Caponiti, Office of Fissile Materials Disposition, U. S. Department of Energy, MD-3, 1000 Independence Avenue SW, Washington DC 20585
47. K. Chidester, Los Alamos National Laboratory, MS-E502, P.O. Box 1663, Los Alamos, NM 87545
48. W. Danker, U. S. Department of Energy, MD-3, 1000 Independence Avenue SW, Washington DC 20585
49. T. Gould, Lawrence Livermore National Laboratory, P.O. Box 808, MS-L186, Livermore, CA 94551
50. L. Jardine, Lawrence Livermore National Laboratory, P.O. Box 808, MS-L166, Livermore, CA 94551
51. Dr. Alexander Kalashnikov, Institute of Physics and Power Engineering, 1 Bondarenko Square, Obninsk, Kaluga Region, Russia 249020
- 52-57. D. E. Klein, Associate Vice Chancellor for Special Engineering Programs, The University of Texas System, 210 West Sixth Street, Austin, TX 78701
58. J. O. Nulton, Office of Fissile Materials Disposition, U.S. Department of Energy, MD-3, 1000 Independence Avenue SW, Washington, DC 20585
59. S. L. Passman, Sandia National Laboratories, 1401 Wilson Blvd., Suite 1050, Arlington, VA 22209
- 60-65. Dr. Alexander Pavlovitchev, Russian Research Center "Kurchatov Institute", Institute of Nuclear Reactors VVER Division, VVER Physics Department, 123182, Kurchatov Square, 1, Moscow, Russia
66. K. L. Peddicord, Associate Vice Chancellor, Texas A&M University, 120 Zachry, College Station, TX 77843-3133
67. G. Radulescu, Framatom Cogema Fuels, 1261 Town Center Drive, MS-423, Las Vegas, Nevada 89143
68. W. D. Reece, Texas A&M University, Department of Nuclear Engineering, Zachry 129, College Station, TX 77843-3133
69. P. T. Rhoads, Office of Fissile Materials Disposition, U.S. Department of Energy, MD-4, 1000 Independence Avenue SW, Washington, DC 20585
70. J. Thompson, Office of Fissile Materials Disposition, U.S. Department of Energy, MD-4, 1000 Independence Avenue SW, Washington, DC 20585
71. M. Yavuz, 7201 Wood Hollow Drive, #475, Austin, TX 78731